

# Decoherence from an Unstable Environment

Robin Blume-Kohout and Wojciech H. Zurek<sup>†</sup>

Los Alamos National Laboratory

(dated: December 13, 2018)

The exponential sensitivity of a quantum environment with a classically chaotic analogue to initial conditions suggests that even very small perturbations resulting from weak coupling to a system whose state is a superposition of eigenstates of the coupling Hamiltonian will compel the environment to evolve into very different states, dependent on the initial state of the system. In this letter, we analyze decoherence due to a "toy" quantum environment which is analytically solvable, yet displays the crucial phenomenon of sensitivity to perturbation. We show that such an environment, with a single degree of freedom, can be far more effective at decohering a harmonic oscillator than a heat bath with infinitely many degrees of freedom. In order to demonstrate this, we introduce a new method of obtaining the master equation for coupled linear systems. Finally, we indicate the shortcomings of our toy model, explain where it differs from physical systems, and comment on the applicability of our results to decoherence caused by a quantum environment with a classically chaotic Hamiltonian.

## I. INTRODUCTION AND MOTIVATION

Classically chaotic systems display a phenomenon known as sensitive dependence on initial conditions. Two copies of such a system, prepared in nearly identical states (two distinct points in phase space, separated by a very small distance), will evolve over time into widely separated states. In an idealized case, the distance between the two points in phase space grows as  $e^{\lambda t}$ , where  $\lambda$  is the largest Lyapunov exponent of the system. This phenomenon does not have a perfect analogue in quantum mechanics, for the simple reason that quantum mechanics is linear; thus "nearly identical" states remain nearly identical for all time! However, Peres [1] predicted an analogous phenomenon for quantum systems: two nearly identical systems, prepared in identical states but obeying slightly different Hamiltonians (i.e.,  $\hat{H}$  and  $\hat{H} + \hat{H}'$ ), will evolve into two different states whose inner product decays exponentially in time when  $\hat{H}$  is classically chaotic. In other words, the Peres Conjecture states that quantum chaos is distinguished by sensitive dependence on the Hamiltonian.

Our interest in this behavior stems from a simple model of decoherence [2], the process by which superposition states evolve into mixtures due to interaction with an environment [3]. A simple but general model of decoherence is generated by an overall Hamiltonian  $\hat{H}_S + \hat{H}_E + \hat{H}_{SE}$ , where the interaction Hamiltonian  $\hat{H}_{SE}$  is a product of a system operator  $\hat{S}$  and an environment operator  $\hat{E}$  (or a sum of such terms). When the system is in an eigenstate  $|j\rangle$  of  $\hat{S}$ , then the environment evolves according to an effective Hamiltonian  $\hat{H}_E + s_j \hat{E}$ . More generally, the system will be in a superposition of the eigenstates of  $\hat{S}$ , in which case the environment experiences a Hamiltonian that is conditional on the state of the system. Thus, if the initial (unentangled) state of the supersystem is  $|\Psi\rangle = \sum_n |j_n\rangle |j_n(0)\rangle$  (where  $|j_n(0)\rangle$  is simply the initial state of the environment), then after a time  $t$ , the state will become  $|\Psi\rangle = \sum_n |j_n(t)\rangle |j_n(t)\rangle$ , where  $|j_n(t)\rangle$  is the state into which the environment evolves if the system is in state  $|j_n\rangle$  (equation 1). When  $\langle j_n(t) | j_m(t) \rangle = 1$ , then no entanglement occurs, the system remains in a pure state, and there is no decoherence. When, however,  $\langle j_n(t) | j_m(t) \rangle \neq 1$ , superpositions of  $|j_n\rangle$  and  $|j_m\rangle$  are transformed into completely decohered mixtures.

This model is tremendously simplified (it ignores many important phenomena, including the effect of the system Hamiltonian). However, it illustrates a key point: the rate at which an environment induces decoherence in a system depends on the decay rate of the overlap  $\langle j_n(t) | j_m(t) \rangle$ , where

$$|j_j(t)\rangle = \exp(-i(\hat{H}_E + s_j \hat{E})t) |j_j(0)\rangle \quad (1)$$

Thus, we expect that the sensitivity of a chaotic environment's Hamiltonian to perturbation will result in rapid decoherence even for very weak coupling.

<sup>†</sup>Electronic address: rbk@socrates.berkeley.edu

<sup>†</sup>Electronic address: whz@lanl.gov

A well-known feature of completely chaotic classical systems is that at every point in phase space there exist stable and unstable manifolds (directions along which a cell respectively shrinks and grows exponentially). These manifolds fold in phase space, enabling a given region to be always stretching in some direction, yet remain within a bounded volume. We examine a system which exhibits such an exponential sensitivity to initial conditions, yet is analytically solvable: the inverted harmonic oscillator. We note that our model does not exhibit folding; we shall comment on the consequences of this shortcoming in due course.

## II. ANALYSIS OF THE UNSTABLE OSCILLATOR

The Hamiltonian for an inverted oscillator is  $H = \frac{p^2}{2M} - \frac{M\omega^2 x^2}{2}$ , where we have replaced the parameter  $\omega^2$  for a simple harmonic oscillator (SHO) with  $-\omega^2$ . Such an "oscillator" does not oscillate at all; it has an unstable fixed point at  $x = 0; p = 0$ , but accelerates exponentially away from the fixed point when perturbed. The price we pay for a solvable system which displays such sensitivity is that its phase space is unbounded; the kinetic energy of the system grows exponentially in time, with a rate determined by  $\omega$ . Although such a system is clearly nonphysical, we believe that on short time scales it can reproduce some of the behavior of a chaotic environment. This "integrable model of chaos" has been used previously [4], in a different context.

We consider an inverted harmonic environment (IHE) consisting of one such oscillator, and couple it to a system consisting of a single SHO with mass  $m$  and frequency  $\omega$ . This supersystem is linear, so it can be analyzed with the same master equation techniques used to treat quantum Brownian motion (QBM) and other linear problems. We will briefly discuss the novel method we use to obtain the coefficients of the master equation.

### A. Obtaining the Coefficients of the Master Equation

We begin with the standard master equation for a linear system coupled linearly to a linear environment (as derived in [5], [6], [7], etc),

$$\frac{\partial \rho}{\partial t} = \frac{1}{i\hbar} \left[ \frac{m\omega^2}{2} x^2, \rho \right] + \frac{1}{2m} [p^2, \rho] + \frac{\kappa}{2} [\rho, \hat{p}] + \frac{\gamma}{2} [\rho, \hat{x}] + f_1(t) [\rho, \hat{x}] + f_2(t) [\rho, \hat{p}] \quad (2)$$

This form is exact when all the terms in  $H = H_S + H_E + H_{SE}$  are linear and quadratic in positions and momenta, provided that the coupling terms in  $H_{SE}$  involve only position operators. Here and throughout, we use  $x$  and  $p$  to denote the position and momentum of the system, and  $y_i$  and  $q_i$  for those of the  $i$ th environmental degree of freedom. To analyze a particular system-environment combination, we need to obtain the specific values of the time-dependent coefficients  $\kappa$ ;  $\gamma$ ;  $f_1$ , and  $f_2$ .

Since the Heisenberg equations of motion for the system and environment operators match exactly the classical equations of motion for the equivalent variables, we can obtain the coefficients of the master equation from its classical analogue, the equation of motion for the reduced system. The supersystem is linear and Hamiltonian, so we can write its trajectories as

$$\mathbf{z}(t) = T \mathbf{z}(0); \quad (3)$$

where  $\mathbf{z}$  is a  $2N$ -dimensional vector of the form  $[x; p; y_1; q_1; y_2; q_2; \dots]$  and  $T$  is a square  $2N \times 2N$  matrix. An equation of motion gives the derivatives of  $\mathbf{z}(t)$  in terms of  $\mathbf{z}(t)$  itself. We obtain this by first differentiating equation (3) to obtain  $\dot{\mathbf{z}}(t) = T \dot{\mathbf{z}}(0)$ , then substituting the  $\mathbf{z}(0)$  obtained by inverting equation (3);  $\mathbf{z}(0) = T^{-1} \mathbf{z}(t)$ . This yields

$$\dot{\mathbf{z}}(t) = T^{-1} \mathbf{z}(t) \quad (4)$$

This is an equation of motion for the supersystem; it gives derivatives of all the supersystem coordinates and momenta in terms of their values at time  $t$ . When we trace over the environment to obtain the master equation, we assume that information about the environment at time  $t$  is unavailable; we know only its initial state. We need a different equation, which respects this constraint.

To obtain an equation of motion that provides  $\dot{x}(t)$  and  $\dot{p}(t)$  in terms of  $x(t)$ ;  $p(t)$ , and the initial state of the environment, we define a new matrix  $T_p$  related to  $T$ :

$$(T_p)_{ij} = \begin{cases} T_{ij} & \text{for } i \leq 1; j \leq 2 \\ 0 & \text{for } i > 2 \end{cases} \quad (5)$$

As we evolve the quantum state of the system, we presume that at all times we have access to knowledge of (1) the reduced density matrix of the system, and (2) the initial state of the environment. The corresponding classical state of knowledge is a vector  $\mathbf{z}_p(t) = [x(t); p(t); y_1(0); q_1(0); \dots]$ . This vector can be obtained using  $T_p: \mathbf{z}_p(t) = T_p \mathbf{z}_p(0)$ . By the same process that led to equation (4), we conclude

$$\mathbf{z}_p(t) = T_p T_p^{-1} \mathbf{z}_p(0) \quad (6)$$

This yields  $\underline{x}(t)$  and  $\underline{p}(t)$ , but in order to obtain the coefficients in the master equation, we need the derivatives of higher order powers of  $x$  and  $p$ . This requires some simplifying assumption; throughout this paper, we will choose to assume that all states are Gaussian. This is particularly convenient since Gaussian states form a closed set under linear evolution. Such states are completely described by linear and quadratic expectation values of  $x$  and  $p$ , so to characterize their evolution we need time derivatives of  $x^2$ ,  $p^2$ , and  $xp$  as well as  $\underline{x}$  and  $\underline{p}$ . This is straightforward; we define the symmetric variance tensor  $\hat{V}_p = \mathbf{z}_p \mathbf{z}_p^T$ , which contains all the quadratic combinations of  $x$  and  $p$ , and transform it as  $\hat{V}_p(t) = T_p \hat{V}_p(0) T_p^T$ . The time derivative of  $\hat{V}_p$  is given by:

$$\dot{\hat{V}}_p = T_p T_p^{-1} \dot{\hat{V}}_p + \hat{V}_p T_p T_p^{-1} \quad (7)$$

Now, we need to relate these quantities to the coefficients of the master equation. For any time-dependent quantum operator  $\hat{A}$ ,  $\frac{d}{dt} \langle \hat{A} \rangle = \text{Tr} \dot{\hat{A}}$ . The derivatives of the relevant expectation values are obtained from the master equation:

$$\frac{d \langle x \rangle}{dt} = \frac{\langle p \rangle}{m} \quad (8)$$

$$\frac{d \langle p \rangle}{dt} = -m \langle x \rangle - \langle p \rangle + F(t) \quad (9)$$

$$\frac{d \langle x^2 \rangle}{dt} = \frac{2}{m} \langle \{x, p\} \rangle \quad (10)$$

$$\frac{d \langle p^2 \rangle}{dt} = 2m \langle \{x, p\} \rangle - 2 \langle p^2 \rangle + 2F(t) \langle p \rangle + 2\tilde{f}_1(t) \quad (11)$$

$$\frac{d \langle \{x, p\} \rangle}{dt} = -m \langle x^2 \rangle + \frac{1}{m} \langle p^2 \rangle - \langle \{x, p\} \rangle + F(t) \langle x \rangle + \tilde{f}_2(t) \quad (12)$$

We can apply the preceding classical analysis to the Heisenberg operators, then equate the results with those from equations (8-12). Equations (8-12) imply that the matrix  $T_p T_p^{-1}$  that gives the derivatives of the Heisenberg operators must take the form

$$T_p T_p^{-1} = \begin{pmatrix} 0 & 0 & 1/m & 0 & 0 & \dots & 1 \\ 0 & m \langle x^2 \rangle & 0 & F_{y1} & F_{q1} & \dots & 0 \\ 0 & 0 & 0 & 0 & 0 & \dots & 0 \\ 0 & 0 & 0 & 0 & 0 & \dots & 0 \\ \vdots & \vdots & \vdots & \vdots & \vdots & \ddots & \vdots \end{pmatrix}; \quad (13)$$

where  $F(t) = \sum_i F_{yi} \langle y_i \rangle + \sum_i F_{qi} \langle q_i \rangle$ . Using this matrix in equation (7) yields the time derivatives of the system variances  $\langle x^2 \rangle$ ,  $\langle p^2 \rangle$ , and  $\langle \{x, p\} \rangle$ :

$$\frac{d \langle x^2 \rangle}{dt} = (V_p)_{11} = \frac{2}{m} \langle \{x, p\} \rangle \quad (14)$$

$$\frac{d \langle p^2 \rangle}{dt} = (V_p)_{22} = 2m \langle \{x, p\} \rangle - 2 \langle p^2 \rangle + F^D(t); pg^E \quad (15)$$

$$\begin{aligned} \frac{d \langle \{x, p\} \rangle}{dt} &= \frac{(V_p)_{12} + (V_p)_{21}}{2} \\ &= -m \langle x^2 \rangle + \frac{1}{m} \langle p^2 \rangle - \langle \{x, p\} \rangle + \frac{1}{2} F^D(t); xg^E \end{aligned} \quad (16)$$

where we've defined  $F^D = \sum_i F_{yi} y_i + \sum_i F_{qi} q_i$ , so that  $F^E = F$ .



$$\omega_{eff}^2 = \frac{\omega_0^2 \dots}{\omega_0^2} \tag{24}$$

$$\omega_{eff} = \frac{\omega_0 \dots}{\omega_0} \tag{25}$$

$$F_{yn} = P \frac{m_0 m_n \dots}{m_0 m_n} \omega_{eff}^2 \tag{26}$$

$$F_{qn} = \frac{m_0}{m_n} \omega_{eff}^2 \tag{27}$$

$$\sim^2 f_1 = \frac{r}{m_i} \sum_{i=1}^N \frac{h}{m_i F_{y_{i-1}} (Y_i)^2 + m_i F_{q_{i-1}} + F_{y_{i-1}} (Y_i q_i) + F_{q_{i-1}} (q_i)^2} \tag{28}$$

$$\sim^2 f_2 = \frac{r}{m_i} \sum_{i=1}^N \frac{h}{m_i F_{y_{i-1}} (Y_i)^2 + m_i F_{q_{i-1}} + F_{y_{i-1}} (Y_i q_i) + F_{q_{i-1}} (q_i)^2} \tag{29}$$

B. Master Equation for the Inverted Harmonic Oscillator

We begin with the supersystem Hamiltonian:

$$H = \frac{p^2}{2m_s} + \frac{m_s}{2} x^2 + \frac{q^2}{2m_e} + \frac{m_e}{2} y^2 + P \frac{m_s m_e}{m_s m_e} xy \tag{30}$$

The time translation matrix T is obtained by diagonalizing the equations of motion, which yields two normal modes. This transformation is characterized by a new harmonic frequency  $\omega$ , a new inverse frequency  $\omega^{-1}$ , and a mixing angle  $\theta$ :

$$\omega^2 = \frac{1}{2} (\omega_0^2 + \omega_e^2) + \frac{q}{(\omega_0^2 + \omega_e^2)^2 + 4g^4} \tag{31}$$

$$\omega^{-2} = \frac{1}{2} (\omega_0^2 + \omega_e^2) - \frac{q}{(\omega_0^2 + \omega_e^2)^2 + 4g^4} \tag{32}$$

$$\tan \theta = \frac{1}{2} \frac{q}{(\omega_0^2 + \omega_e^2)^2 + 4g^4} \tag{33}$$

$$\tag{34}$$

Using these quantities, the  $T_p$ -matrix can be expressed in the form of equation (22), where the  $\phi_i(t)$  are given by:

$$\phi_0(t) = \cos^2 \frac{\sin(\omega t)}{\omega} + \sin^2 \frac{\sinh(\omega^{-1} t)}{\omega^{-1}} \tag{35}$$

$$\phi_1(t) = \frac{\sin 2\theta}{2} \frac{\sin(\omega t)}{\omega} - \frac{\sinh(\omega^{-1} t)}{\omega^{-1}} \tag{36}$$

Thus, for this case we immediately obtain the parameters of the master equation by direct substitution into equations (24-29). All terms share a common denominator, which we denote by D:

$$D = \omega^2 \cos^2 \sin^2 \sin(\omega t) \sinh(\gamma t) + \omega^2 \cos(\omega t) \cosh(\gamma t) \cos^2 \sin^2 + \cos^4 + \sin^4 \quad (37)$$

$$\omega_{\text{eff}}^2 = \frac{\omega^2}{D} \left[ \omega^2 \cos^4 \sin^2 + \frac{\sin^2 2}{4} \omega^2 \cos(\omega t) \cosh(\gamma t) - 2 \sin(\omega t) \sinh(\gamma t) \right] \quad (38)$$

$$\omega_{\text{eff}} = \frac{\omega^2 + \sin^2 2}{4D} \left[ \sin(\omega t) \cosh(\gamma t) - \cos(\omega t) \sinh(\gamma t) \right] \quad (39)$$

$$F_y = \frac{P}{m_s m_e} \frac{\omega^2 + \sin^2 2}{2D} \cos^2 \cosh(\gamma t) + \sin^2 \cos(\omega t) \quad (40)$$

$$F_q = \frac{r}{m_e} \frac{\omega^2 + \sin^2 2}{2D} \cos^2 \sinh(\gamma t) + \sin^2 \sin(\omega t) \quad (41)$$

We separate the diffusion coefficients into portions proportional to the three variances which describe the initial environment state:  $f_1 = f_1^{yy} (y^2) + f_1^{yq} (yq) + f_1^{qq} (q^2)$  and  $f_2 = f_2^{yy} (y^2) + f_2^{yq} (yq) + f_2^{qq} (q^2)$ . Factoring out the common prefactor  $\frac{m_s}{4\omega^2 D} \sin^2 2 \omega^2 + \sin^2$ , we obtain:

$$f_1^{yy} = m_e \left[ \cos^2 \cosh(\gamma t) + \sin^2 \cos(\omega t) (\sinh(\gamma t) + \sin(\omega t)) \right] \quad (42)$$

$$f_1^{yq} = \frac{\omega^2 \cosh(\gamma t) + \sin^2 \cos(\omega t) (\cosh(\gamma t) - \cos(\omega t))}{\omega^2 \sinh(\gamma t) + \sin^2 \sin(\omega t) (\sinh(\gamma t) + \sin(\omega t))} \quad (43)$$

$$f_1^{qq} = \frac{\omega^2 \sinh(\gamma t) + \sin^2 \sin(\omega t) (\cosh(\gamma t) - \cos(\omega t))}{m_e} \quad (44)$$

$$f_2^{yy} = m_e \left[ \cos^2 \cosh(\gamma t) + \sin^2 \cos(\omega t) (\cosh(\gamma t) - \cos(\omega t)) \right] \quad (45)$$

$$f_2^{yq} = \frac{\cos^2 \cosh(\gamma t) + \sin^2 \cos(\omega t) (\sinh(\gamma t) - \sin(\omega t))}{\omega^2 \sinh(\gamma t) + \sin^2 \sin(\omega t) (\cosh(\gamma t) - \cos(\omega t))} \quad (46)$$

$$f_2^{qq} = \frac{\omega^2 \sinh(\gamma t) + \sin^2 \sin(\omega t) (\sinh(\gamma t) - \sin(\omega t))}{m_e} \quad (47)$$

### III. RESULTS AND ANALYSIS

Having obtained a master equation describing the evolution of a system coupled to an IHE (inverted harmonic environment), we now proceed to examine the consequences of that evolution. We have two tools for this analysis: on one hand, the master equation and its coefficients determine the instantaneous effects of the environment; on the other hand, we can explicitly evolve an initial state of the system to see the time evolution of state properties such as entropy and energy. The master equation itself divides naturally into two parts corresponding to the two lines of equation 2; the terms in the first line produce renormalized unitary evolution (including external damping and forcing terms, which break unitarity), while the last two terms are dissipative and responsible for decoherence. We thus divide our analysis into three sections, addressing in turn the quasi-unitary portion of the master equation, the dissipative terms in the master equation, and the behavior of evolved observables. Our primary results are in equations 60-61, where we demonstrate the linear rate of entropy growth in the system and obtain an approximate decoherence timescale which is logarithmically dependent on the coupling. Thus, the reader who wishes to skip straight to the meat of the subject should skim most of sections IIIA and IIIB, which analyze in detail the behavior and pathology of the master equation.

## A . Unitary evolution

The first few terms in the right-hand side of equation 2,

$$\frac{1}{i\hbar} \frac{m \omega_{\text{eff}}^2}{2} \hat{x}^2 + \frac{1}{2m} \hat{p}^2 + \frac{\omega_{\text{eff}}}{2} [\hat{x}; \hat{p}; \hat{g}] F(t) [\hat{x}; \hat{p}] \quad (48)$$

are exactly those for the evolution of an isolated harmonic oscillator subject to an external force  $F(t)$  and a damping force  $\omega_{\text{eff}}(t)$ . For convenience, although the term  $\omega_{\text{eff}} [\hat{x}; \hat{p}; \hat{g}]$  breaks unitarity, we refer to these terms in the master equation as the "unitary evolution" terms.

Because the coefficients of all the terms except  $\hat{p}^2$  are time-dependent, however, the evolution induced by these terms is not necessarily intuitive. The time-dependence of  $\omega_{\text{eff}}^2$  and  $\omega_{\text{eff}}$  (for various values of parameters) is shown in Figure 1; the base configuration is  $m_s = m_e = 1$ ,  $\omega = 10^3$ . We see immediately that although the coefficients are initially very close to their bare values ( $\omega_{\text{eff}}^2 \approx \omega^2$ ,  $\omega_{\text{eff}} \approx \omega$ ), they begin after a certain time to vary dramatically, and finally appear to converge to a periodically diverging function of time. Thus, coefficients which we expect to be positive and well-defined (and which, in the QBM model, settle down after a while to stable values) not only take on negative values, but appear at certain times to become infinite.

The root of this behavior is apparent in the common denominator of all the coefficients (equation 37). This denominator, the determinant of the upper-left  $2 \times 2$  submatrix of  $T_p$ , takes on both positive and negative values (and thus passes through zero). Since the various numerators in equations 38-47 do not change sign in sync with the denominator, all the coefficients not only vary from positive to negative, but diverge whenever  $D = 0$ . While this phenomenon is unexpected and counter-intuitive, we note that it does not indicate unphysical behavior. Detailed analysis (omitted here) shows that near a divergence in the coefficients, the system state is forced to assume a form such that the effects of the superoperators in the master equation cancel each other out; thus, when the coefficients diverge, their effects sum to a perfectly finite value, and the evolution of the state is completely physical.

We conclude from this that the divergences are symptomatic not of any physical phenomenon, but rather of a breakdown in the system-environment paradigm that we have imposed on the supersystem. As the system and environment interact with each other, information about the initial  $x_0$  and  $p_0$  of the system is transferred to the environment (and vice-versa). At certain times, all information about a particular linear combination of  $x_0$  and  $p_0$  has been transferred to the environmental degrees of freedom, in return for which all information about some linear combination of  $y_0$  and  $q_0$  resides in the system degrees of freedom. This is true only for an instant, but at that instant  $\hat{\rho}(t)$  does not uniquely determine  $\hat{\rho}(0)$ , no differential equation for  $\hat{\rho}$  can exist, and the master equation necessarily breaks down. The mathematical reflection of this is that the upper-left  $2 \times 2$  submatrix of  $T_p$  (which specifies the relationship between  $(x;p)$  and  $(x_0;p_0)$ ) is instantaneously non-invertible, which makes  $D = 0$ .

For  $t = 0$ ,  $D = 1$ . Assuming that the coupling is weak ( $\epsilon \ll 1$ ), we can expand  $D$  for  $t \ll \tau_c \approx 2^{-1} \log \epsilon^{-1}$  as

$$D \approx 1 + \frac{2\epsilon^2 t^2 \sin^2(\omega t) + 2\epsilon \cos(\omega t)}{1} \quad (49)$$

Since the fraction at the end of equation 49 is  $O(\epsilon)$ , we conclude that  $D \approx 1$  until shortly before the first divergence occurs; further, the timescale of that divergence is

$$t_c \approx \frac{\log \epsilon^{-1}}{2\omega} + \log \frac{1}{1 + 2\epsilon} \quad (50)$$

While the first divergence may occur later than  $t_c$ , it cannot occur earlier. Thus, we have a natural time scale in the system, which divides time into two regions: short times, when  $t < t_c$ ; and long times, when  $t > t_c$ . In the short-time regime, the unitary coefficients of the master equation are well-approximated by their bare values, whereas in the long-time regime the coefficients' values periodically diverge and are only indirectly related to their bare values. When  $t \approx t_c$ , the coefficients' values are difficult to characterize. Finally, we note that the critical timescale is reflected in the dissipative coefficients as well (see Figure 2), but not necessarily in physical quantities obtained from  $\hat{\rho}(t)$  itself, as we expect from the argument that the divergences are not reflected in physical quantities.

Nonetheless,  $t_c$  is a convenient time scale because in the short-time regime we can be assured that the renormalized unitary evolution is very similar to the bare unitary evolution; thus, the effects of interaction with the environment during this regime will be all but unnoticeable on classical scales. Beyond  $t_c$ , the terms in the master equation which govern the evolution of large-scale structures in phase space may depart dramatically from their uncoupled values; we cannot be certain. If we take, as the criterion for our model's relevance to a real chaotic environment, that its effects be small on classical scales, then relevance is guaranteed for short times, but not for long times. Thus, although we will examine the long time behavior of the model at times, we are primarily concerned with short times.

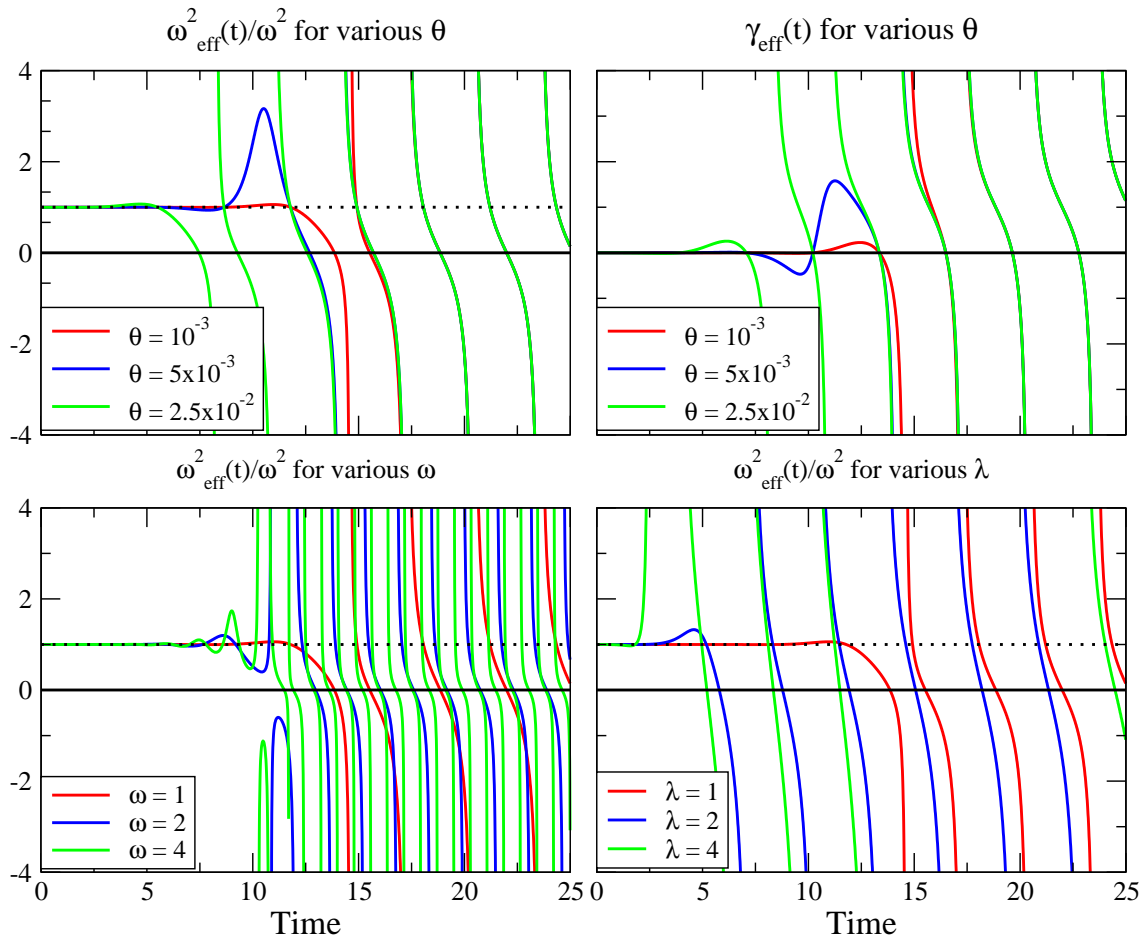


FIG. 1: Dependence of  $\omega_{\text{eff}}^2$  and  $\gamma_{\text{eff}}$  on  $\theta$ ,  $\omega$ , and  $\lambda$ .

Another perspective on the same conclusion comes from the fact that any physical chaotic environment will have a bounded phase space. The operators  $\hat{E}_i$  which couple to system operators  $\hat{S}_i$  will thus have bounded spectra, and the expectation value of the generalized coupling  $\hat{H}_{\text{int}} = \sum_i \hat{S}_i \hat{E}_i$  will also be bounded by some value  $\hat{H}_{\text{int}}^{\text{max}}$ . As long as our model respects this constraint, we can consider it a plausible model for that environment; however, because the  $\hat{Y}$  operator is unbounded and  $\hat{Y}^2$  increases exponentially in time, our model will eventually expand into a larger phase space, and the coupling will dominate the overall Hamiltonian. The critical time  $t_c$  indicates roughly when  $\hat{H}_{\text{int}}$  begins to dominate the overall Hamiltonian.

### B. Dissusive terms

The last two terms in equation 2,

$$f_1(t) [\hat{x}; \hat{x}; \hat{p}] + f_2(t) [\hat{x}; \hat{p}; \hat{p}]; \quad (51)$$

are non-unitary and dissipative, and produce decoherence. If  $\hat{\rho}$  is transformed to a Wigner function  $W(x;p)$  [6], then equation 2 becomes a Fokker-Planck type equation. The  $f_1$  or "normal diffusion" term is seen to produce diffusion in momentum space according to  $W \rightarrow \int f_1 \frac{\partial^2}{\partial p^2} W$ , while the  $f_2$  or "anomalous diffusion" term tends to skew the state according to  $W \rightarrow \int f_2 \frac{\partial}{\partial x} \frac{\partial}{\partial p} W$ . This is also apparent in equations 8-12, where  $f_1$  appears only in  $\frac{\partial \langle \hat{p}^2 \rangle}{\partial t}$  while  $f_2$  appears only in  $\frac{\partial \langle \hat{x} \hat{p} \rangle}{\partial t}$ .

In QBM, the coefficients  $f_1$  and  $f_2$  of these terms equilibrate to constant values or monotonically decreasing functions after an initial period; in our IHE model these coefficients, like those of the unitary terms, vary widely over time.

Unlike those coefficients,  $f_1$  and  $f_2$  are dependent on the state of the environment; however, they can each be written as the contraction of a  $2 \times 2$  coefficient tensor with the variance tensor of the environment at  $t = 0$  (see equations 42-47):

$$f_n(t) = \text{Tr} \begin{pmatrix} f_n^{yy} & \frac{1}{2} f_n^{yq} \\ \frac{1}{2} f_n^{yq} & f_n^{qq} \end{pmatrix} \begin{pmatrix} y^2 & yq \\ yq & q^2 \end{pmatrix} : \quad (52)$$

The absolute values of the three subcoefficients for each of  $f_1$  and  $f_2$  are plotted in Figure 2, for the same base parameters as Figure 1 and three different coupling strengths. Each subcoefficient has a prefactor involving the masses of the system and environment, which is ignored in these plots; thus, if the system and environment masses are substantially different, one subcoefficient may be promoted over another. The most salient feature of these plots is that they appear identical (only at times shorter than  $\tau^{-1}$  is any difference visible at all between the various coefficients). Examination of equations 42-47 confirms that for  $t \ll \tau^{-1}$ , all the subcoefficients are proportional to  $D^{-1} e^{-t}$ . This also explains the sharp distinction between short- and long-time behavior in Figure 2. In the short-time regime,  $D \ll 1$ , and each subcoefficient is well-approximated by  $f / e^{-t}$ ; in the long-time regime, however,  $D \gg 1$ , and  $f \sim e^{-t} \cos(\omega t)$ , and  $f \sim e^{-t} \sec(\omega t)$ . Thus, on the log-plot of Figure 2, we see two distinct lines with slopes  $-2$  and  $0$ , the second of which is punctuated by the periodic divergences seen in all the master equation coefficients. In order to make this explicit, we examine the short-time ( $\tau^{-1} < t < \tau_c$ ) behavior of  $f_1$ , which is responsible for entropy production (see section IIIC), when the mass ratio  $m_{\text{env}} = m_{\text{sys}} \ll 1$ . In this limit,  $f_1$  is dominated by  $f_1^{qq}$ ; using the approximations  $\sinh(\omega t) \approx \omega t$ ,  $\cos(\omega t) \approx 1$  and  $D \ll 1$ , we obtain:

$$f_1 \sim \frac{m_s^2 (\omega^2 + \gamma^2)}{m_e} e^{-t} \quad (53)$$

The key point in equation 53 is that the coefficient of the term which produces diffusion in momentum (the primary factor in decoherence) increases exponentially with time and  $\omega$ , but is only quadratic in the coupling strength.

The change in the exponent of the  $f$  coefficients at  $t = \tau_c$  is physically relevant as well as mathematically sensible. In the short-time regime, the oscillatory dynamics of the system and the hyperbolic stretching of the environment proceed largely independent of each other; just as the environment induces only minor perturbations in the system, the system does not disturb the environment greatly. Thus, the stretching of the environment along its unstable manifold is reflected in the system as diffusion in one of the two phase-space dimensions. After  $\tau_c$ , however, the interaction Hamiltonian begins to dominate the dynamics of the system, the overall dynamics is strongly coupled, and the unstable manifold of the environment rotates. Diffusion in the system is averaged over stable and unstable directions, and so the diffusion coefficients increase only as  $e^{-t}$ . Nonetheless, because diffusion now occurs along all directions in phase space, the entropy of  $\hat{\rho}$  continues to grow at the same rate (as will be shown in section IIIC).

### C. Entropy and Energy of the Reduced Density Matrix

Having analyzed in detail the IHE master equation, we turn finally to the actual behavior of  $\hat{\rho}(t)$ . Because decoherence manifests as entropy production in  $\hat{\rho}$ , we first calculate the Von Neumann entropy  $S(t) = -\text{Tr}(\hat{\rho} \ln \hat{\rho})$  of the reduced density matrix, and examine the dependence of  $S(t)$  on various parameters. However, entropy production can reflect not only the destruction of quantum coherences but also the destruction of large-scale "classical" structures in phase space. In order to verify the ability of the IHE to produce decoherence without destroying classical structures, we take the expectation value of energy  $E = \langle \hat{H}_{\text{sys}} \rangle$  as a convenient classical quantity, and show that for appropriate initial conditions a dramatic rise in  $S$  occurs while  $E$  remains relatively undisturbed. It is worth noting that because all the states we consider have  $\langle x \rangle = \langle p \rangle = 0$ , this is probably an overly strong condition, since large (on classical scales) amounts of energy can be added to the system by a simple Galilean transformation at  $t = 0$ , which changes nothing of the analysis except for adding a constant offset to  $E(t)$ .

#### 1. Entropy

The canonical state to examine is a "Schrodinger Cat" state, typically a superposition of widely separated coherent states. We have examined the effects of the IHE on such a state, but because the state is not itself Gaussian the analysis is quite messy in our ansatz, and so we will discuss instead the behavior of a Gaussian state which is highly extended in  $x$ . With respect to a diffusive decoherence process, the most significant features of a "cat" state are the interference fringes in  $W(x;p)$  which lie between the two Gaussian bumps, and which are highly extended in  $x$  but

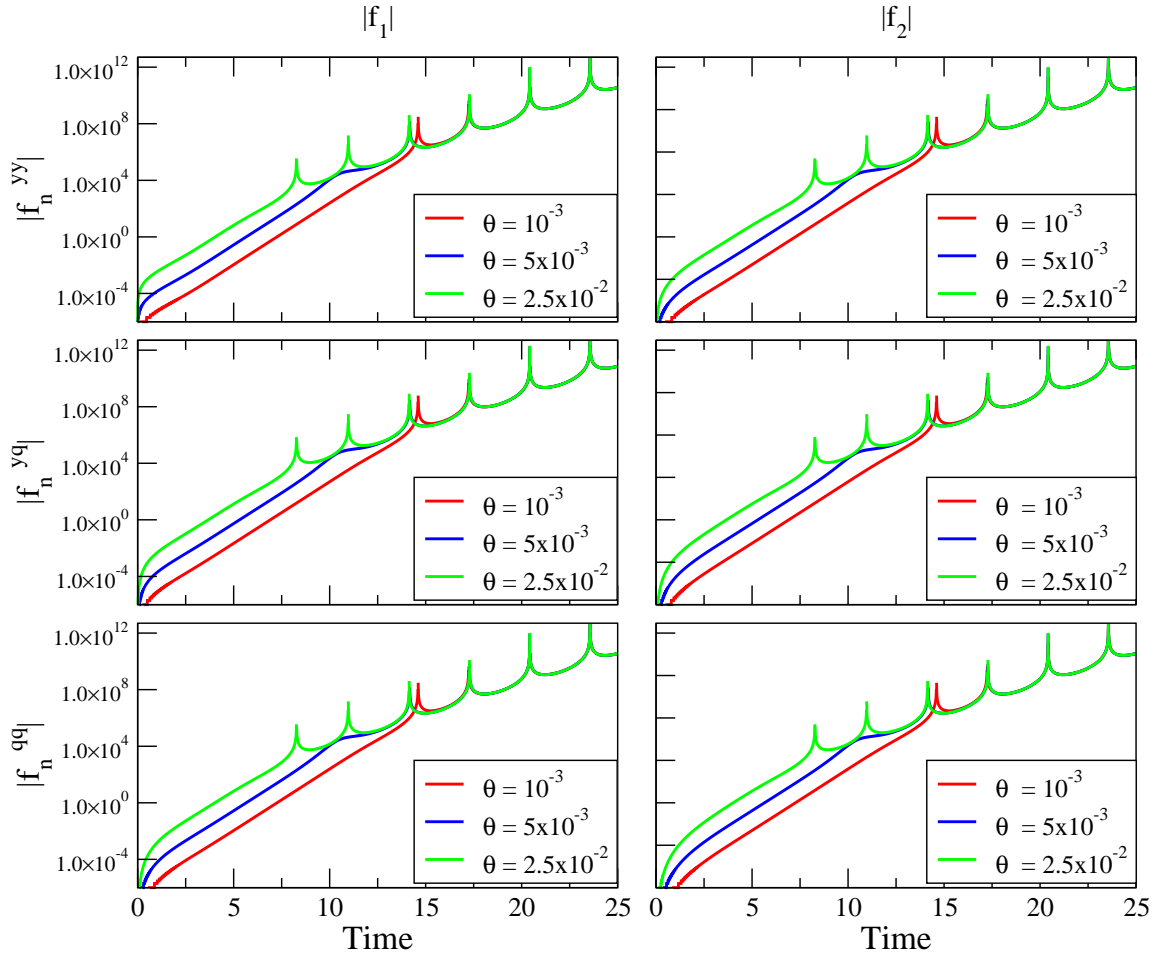


FIG. 2: Dependence of the diffusion coefficients  $f_n(t)$  on  $\theta$ .

equivalently narrow in  $p$ . A Gaussian state which is highly squeezed in momentum has similar small-scale structure, reflected in strong off-diagonal correlations in  $\hat{\rho}$ . For convenience, we consider such states.

In general,  $\text{Tr}(\hat{\rho} \log \hat{\rho})$  is difficult to compute. For Gaussian states, however,  $S$  can be easily computed in terms of the state's scaled area in phase space. The Heisenberg uncertainty relation  $\Delta x \Delta p \geq \frac{\hbar}{2}$  provides a fundamental unit of phase space area. We thus define  $a_0 = \frac{\hbar}{2}$ , and define the phase space area occupied by a Gaussian state as

$$a = \frac{q}{\Delta x^2 \Delta p^2} = (\Delta xp)^2; \tag{54}$$

and the scaled area as  $A = a/a_0$ . Every Gaussian pure state has an area  $a = a_0$ ; mixed states have  $a > a_0$ . It can be shown that the entropy is given exactly by

$$S = \frac{1}{2} [(A + 1) \ln(A + 1) - (A - 1) \ln(A - 1)] \ln(2); \tag{55}$$

A convenient approximation, which is exact for  $S = 0$  and is always accurate to within  $1 - \ln 2 \approx 0.31$ , is

$$S \approx \ln(A) = \frac{1}{2} \ln(A^2); \tag{56}$$

where the second equality is convenient because  $A^2$  is easily calculable as the determinant of the state's variance tensor.

## 2. Analysis of the $S(t)$ Plots

In Figures 3 and 4,  $S(t)$  is plotted for a wide range of initial conditions and parameters. The initial conditions consist of the squeezing parameter  $r$  and squeezing angle  $\phi$  for both the system and the environment (large  $r$  and  $\phi = 0$  indicates a state extended in position and squeezed in momentum, while  $\phi = \frac{\pi}{2}$  implies the reverse). The parameters of the master equation include the bare  $\lambda$  and  $\mu$ , the coupling  $\gamma$ , and mass-ratio  $\alpha = m_e/m_s$ . The base parameters used in Figures 3 and 4 are:  $\lambda = 1$ ,  $\mu = 1$ ,  $\gamma = \frac{1}{64}$ ,  $m_s = 1$ ,  $m_e = 1$ ,  $r_s = 4$ ,  $r_e = 2$ ,  $\phi_s = 0$ , and  $\phi_e = 0$ . Each of the plots varies one of these parameters.

All eight plots demonstrate the same basic behavior: entropy increases linearly as  $S = \gamma t + S_0$ , with periodic modulations. The last plot in Figure 4 demonstrates the dependence on  $\alpha$ , with the intriguing caveat that for  $\alpha = 0$  we obtain not constant entropy, but logarithmically increasing entropy. This is explained by the fact that for  $\alpha = 0$  the environment is a free particle, whose wavepacket spreads as  $\langle y^2 \rangle / t$ ; this mild irreversibility produces entropy growth which is only asymptotically zero. For other values of  $\alpha$ ,  $\langle y^2 \rangle / e^{2\gamma t}$ , and entropy grows linearly.

Varying the squeezing parameter or squeezing angle of the environment (Figure 3) changes only the initial jump in entropy,  $S_0$ .  $S_0$  is minimal for an unsqueezed environment ( $r_e = 1$ ), and increases approximately as  $\log(r_e + r_e^{-1})$ . The dependence on  $\phi_e$  is minimal for  $\alpha = 1$ ; for larger or smaller mass ratios, the dependence on the squeezing angle becomes more noticeable. It should be noted that the phrase "initial jump in entropy" refers precisely to the intercept of  $S(t) \sim \gamma t + S_0$  in the long time limit;  $S_0$  can be negative, which means only that the linear growth in entropy is postponed for a time  $-S_0/\gamma$ .

Also in Figure 3, it is apparent that the effect of varying  $r_s$  and  $\phi_s$  is merely to modify the periodic modulation of  $S(t)$ . Since the system state rotates in phase space (according to the dynamics) over time anyway, changing  $\phi_s$  merely changes the phase of the oscillation in  $S(t)$ , while  $r_s$  determines the shape and amplitude of the oscillation: it becomes more dramatic as  $r_s$  increases or decreases from 1 (which eliminates the modulation).

Figure 4 shows the effects of varying  $\lambda$ ,  $\mu$ ,  $\gamma$ , and  $\alpha$ . Both  $\lambda$  and  $\mu$  affect  $S$  without changing the character of  $S(t)$  in any other way. This is particularly interesting for the coupling  $\gamma$ ; regardless of how small the coupling is, the entropy still grows as  $e^{\gamma t}$ . In particular, the plot for  $\gamma = \frac{1}{1024}$  corresponds to a crossover time of  $t_c > 15$ , yet entropy begins to grow linearly around  $t = 2.5$ . Changing  $\mu$ , as mentioned earlier, changes the rate of entropy production. Finally, the result of varying  $\lambda$  is a change in the periodic modulation; the frequency of this modulation is of course  $\lambda$ . Of special interest is the curve for  $\lambda = 0$ ; here, although the periodic modulation has vanished,  $S(t)$  rises not as  $t$  but as  $t + \log(t)$ . The explanation is the same as it was for the  $\alpha = 0$  case; when  $\lambda = 0$  the system is a free particle, and the linear spread of  $x^2$  contributes a logarithmic term to the entropy.

## 3. Conclusions regarding Entropy and Energy

The linear growth of entropy seen in Figures 3 and 4 indicates that the IHE model can continue to decohere a system to which it is coupled after other models, such as QBM, have saturated. However, it does not demonstrate that the IHE can produce decoherence faster than QBM. To examine this issue, we first derive a formula for the rate of entropy growth.

The exact entropy (equation 55) is difficult to work with; therefore we approximate  $S(t)$  with  $S'(t)$  from equation 56. Using equations (8-12)), we obtain

$$\frac{\partial}{\partial t} (A^2) = -\gamma_{\text{eff}}(t)A^2 + 2f_1(t)x^2 - f_2(t)\langle \text{hfx} \rangle; \text{pg}=2i; \quad (57)$$

where  $S'(t) = \frac{1}{2} \log A^2$ . Not surprisingly, a positive dissipation coefficient  $\gamma_{\text{eff}}$  causes the state to shrink in phase space; however, as we saw in the analysis of the unitary term  $s$ ,  $\gamma_{\text{eff}}$  can be both positive and negative, and thus expands the state as often as it shrinks it. We conclude that the  $\gamma_{\text{eff}}$  term contributes only to the periodic modulation of  $S(t)$ . The effect of the  $f_2$  term is highly dependent on  $\langle \text{hfx} \rangle; \text{pg}=2i$ , which can be positive, negative, or zero. However, because  $\langle \text{hfx} \rangle; \text{pg}=2i$  oscillates around 0 as the system evolves, this term will contribute primarily to the periodic modulation as well. This leaves:

$$\frac{\partial}{\partial t} (A^2) \sim 2f_1(t)x^2 \quad (58)$$

Since  $x^2$  is strictly positive and  $f_1(t)$  in the short-time regime  $t < t_c$  is positive (see equation 53), this predicts monotonic growth in  $A^2$ , and thus  $S(t)$ . In addition, we can use the previous analysis of  $f_1(t)$  to approximate

$$f_1(t) \sim \gamma^2 e^{2\gamma t} \quad (59)$$

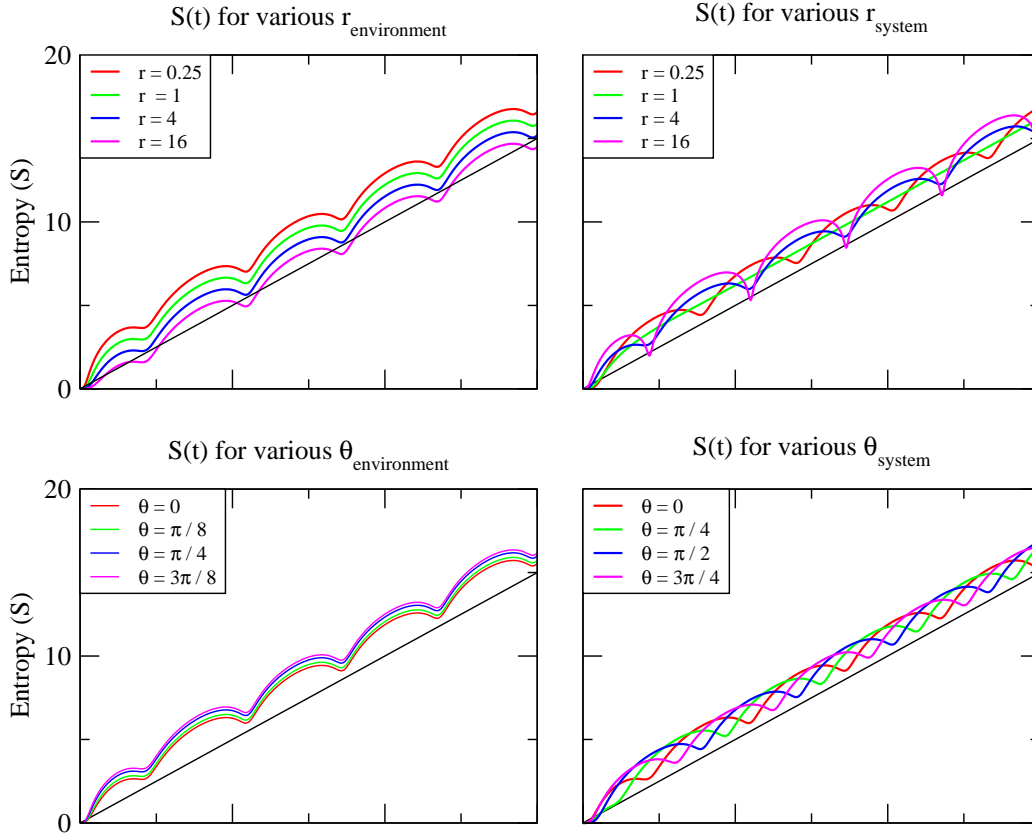


FIG. 3: Dependence of system entropy on initial states of the system and the environment.

(where  $\alpha$  depends on  $\gamma$ ,  $\beta$ ,  $\theta$ , and the initial state of the environment, but not on time) and integrate equation 58, obtaining

$$S(t) = \log(\alpha^2) + \log \beta + \alpha t \quad (60)$$

This equation summarizes our most significant results. The amount of entropy produced in time  $t$  is linear in time and  $\alpha$ , but only logarithmically dependent on the properties of the environment or the coupling strength. We can invert equation 60 to obtain an approximate decoherence time  $t_d$ , which is the time required to produce a certain amount  $S_0$  (e.g., 1 bit for a Schrödinger Cat state) of entropy from an initial pure state:

$$t_d \approx \frac{1}{\alpha} (S_0 - \log(\alpha^2) - \log \beta) \quad (61)$$

The key point is that  $t_d$  is inversely linear in  $\alpha$ , but only logarithmic in the coupling  $\gamma$  or the initial properties of the environment (contained in  $\beta$ ). As the coupling becomes very weak, then, we expect only moderate increases in the decoherence time. This should be contrasted with QBM, where the decoherence time has a power-law dependence on the coupling strength, so that extremely weak couplings can lead to arbitrarily long decoherence times.

Finally, we consider the system's energy. If there is no coupling to the environment, then  $E$  is a constant of the motion; conversely, when  $E$  is substantially disrupted, we can no longer regard the environment as a classically perturbative influence. Since the system energy is given by

$$E(t) = \frac{1}{2} m_s \dot{x}^2 + \frac{1}{m_s} p^2 \quad ; \quad (62)$$

we can immediately calculate its time derivative as

$$\frac{\partial E}{\partial t}(t) = \frac{f_1(t) \cdot p^2}{m_s} \quad (63)$$

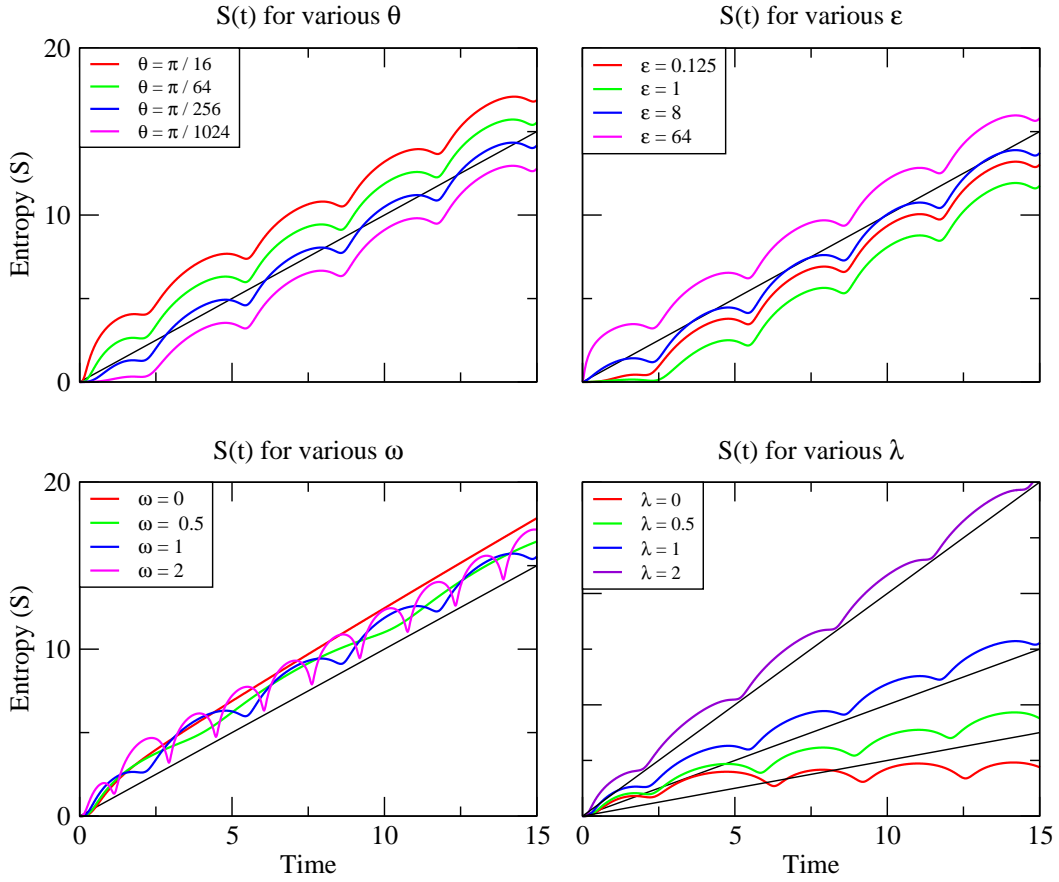


FIG. 4: Dependence of system entropy on parameters of the master equation.

Clearly  $E$  will grow, because of the  $f_1(t)$  term. However,  $\frac{\partial A^2}{\partial t}$  also contains  $f_1$ , but multiplied by  $x^2$ . Thus, for states which are highly squeezed in momentum, rapid growth in  $S$  is achieved relative to the growth in  $E$ . In addition,  $E(0)$  (the initial energy of the system) plays no role in  $\frac{\partial E}{\partial t}$ ; thus, if the initial energy of the system is high, the added energy  $E(t) - E(0)$  will be negligible in comparison for some period of time. We conclude that for initial states which have large  $x^2$  and large  $E(0)$  (i.e., superposition states over classical length scales), a relatively long period of time exists over which energy growth is negligible, while entropy grows rapidly. An example is given in Figure 5.

#### IV. CONCLUSION

We emphasize again not only that the system we have studied is a non-physical, oversimplified model for a chaotic environment, but that our analysis yields results so complicated that we had to make even more simplifying assumptions at the end in order to get a "thumb nail result" (equation 61). However, the result that we obtain is significant; we have shown that an environment with a single degree of freedom and access to a finite-dimensional Hilbert space can produce decoherence more rapidly than the canonical QBM environment, which requires infinitely many degrees of freedom and an infinitely large Hilbert space. The analysis given necessarily examines a system which has an infinite-dimensional Hilbert space (since the phase space volume of the IHE is unbounded), but we can imagine a system with a bounded phase space which simulates an inverted oscillator arbitrarily well up to a certain time. Such a system would produce the same results over the time of interest, but would not be analytically soluble beyond that time.

A brief comment is in order on the principle which enables our "small" (in terms of degrees of freedom and available Hilbert space dimension) environment to be so effective. A good measure of an environment's decohering efficacy is the amount of entropy it can produce in the system, and the rate at which that entropy is produced. For pure initial states of the environment, entropy can only be produced through entanglement; the total entropy which can be produced is limited by  $\log_2(D \text{ in } [\mathbb{H}_{env}])$ . Thus, in the long run larger environments can decohere more effectively. The rate at which the entropy is produced, however, is limited by the rate at which the environment can explore its

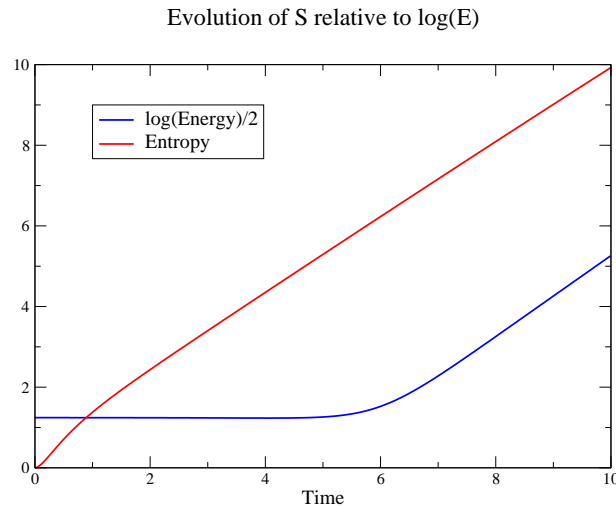


FIG. 5: Comparison of  $S(t)$  and  $E(t)$  for an extended state. We have normalized  $E$  by an arbitrary  $E_0$ ; in addition, since  $E$  grows as  $e^{2t}$ , we have plotted  $\frac{1}{2} \log(E)$  so that both curves have the same slope asymptotically. The noteworthy regime is  $t < 5$ , where the entropy grows steadily but  $\log(E)$  remains virtually constant. The parameters for this calculation are:  $\beta = 10^{-5}$ ,  $\alpha = 1$ ,  $m_s = m_e = 1$ , and  $\gamma = \frac{1}{512}$ . The initial state of the system is squeezed by a factor of  $10^4$ , with the long axis located at an angle of  $\frac{\pi}{4}$  to the  $\hat{x}$ -axis; the environment is initially squeezed by a factor of 16 in  $\hat{p}$ .

phase space. Because a collection of harmonic oscillators is a stable system, small perturbations due to the state of the coupled system do not induce exploration of a large volume of phase space for any one oscillator. The inverted oscillator, on the other hand, can explore its volume much more efficiently when perturbed. Critics may point out that the IHE is an unphysical model; while this is true, the extensively studied QBM model is unphysical for other reasons (one being the lack of a thermalization mechanism within the environment).

We view this work as the first step in a larger project: understanding the role that chaotic systems play in decoherence. These results for the IHE environment clearly show that a particular unstable environment can not only decohere a system in a manner markedly different from the standard (QBM) models of decoherence, but also display unexpected behavior (e.g., the periodic breakdown of the master equation formalism due to singularities in the coefficients). While we believe we have sketched accurately the regime in which our toy model represents faithfully the behavior of actual chaotic environments, the clear next step is to examine such environments directly using numerical simulations, and to see which of these results for the IHE remain unchanged. There remains another extremely important regime which we do not examine here: environments with many chaotic degrees of freedom (the atmosphere of the earth, for instance).

In addition to these obvious future directions, this work raises related questions about the behavior of open systems. The key step in any decoherence process is that of tracing over the environment; if this is not done, the state of the system is an entangled pure state, not a mixed state. This is commonly justified by the argument that the environment is vast (the whole universe, potentially) and this size guarantees that some of the information which has been transferred to the environment has been irreversibly lost. Despite this (reasonable) justification, explicit models of open quantum systems are usually bipartite; there is a small system, and a larger but still small (with respect to the universe) environment to which the system is coupled. If, however, one imagines a set of concentric environments  $E_i$ , each much larger than the last, as a model for the entire universe, then the environment to which the system is coupled ( $E_0$ ) serves not as an independent environment, but rather as a communication channel between the system and the greater universe. In this model, which we intend to investigate, the entropy of the system is not limited by the size of the environment (as it is in the bipartite  $S(E)$  model, but only by its own size; a small local environment can catalyze massive entanglement between the system and the universe. Our analysis of the IHE model indicates that chaotic local environments may be more efficient at carrying information away from the system than integrable environments.

Finally, one of us has examined elsewhere [2, 8] the role of small-scale structures in phase space with respect to decoherence. While this issue is not directly relevant to the IHE (because Gaussian states do not have sub-Planck structures), the IHE appears to be effective at producing entropy in part because it rapidly occupies a highly extended phase space. We intend to explore the role of sub-Planck structure in more detail in the context of actual chaotic environments.

## A cknow ledgm ents

The authors would like to thank Juan Pablo Paz and Bill Unruh, for discussions and ideas. This work was supported in part by a grant from the NSA.

- 
- [1] A. Peres, "Quantum Theory: Concepts and Methods", (Kluwer Academic Publishers, 1995).
  - [2] Z. Karkuszewski, C. Jarzynski, W. H. Zurek, Phys. Rev. Lett. 89, 170405 (2002).
  - [3] J. P. Paz and W. H. Zurek, Environment-induced decoherence and the transition from quantum to classical, in Coherent Matter Waves, Les Houches Session LXXII, edited by R. Kaiser, C. Westbrook, and F. D'avid (Springer Verlag, Berlin, 2001), pp. 533-614.
  - [4] W. H. Zurek and J. P. Paz, Phys. Rev. Lett. 72, 2508 (1994).
  - [5] A. O. Caldeira and A. J. Leggett, Physica 121A, 587 (1983).
  - [6] W. G. Unruh and W. H. Zurek, Phys. Rev. D 40, 1071 (1989).
  - [7] B. L. Hu, J. P. Paz, Y. Zhang, Phys. Rev. D 45, 2843 (1992).
  - [8] W. H. Zurek, Nature 412, 712-717 (2001).